

Solid-State Polymerization of 7,7,8,8-Tetrakis(methoxyethoxycarbonyl)-quinodimethane under UV Irradiation

Takahito Itoh,^{*,†} Satoshi Yamashita,[†] Shinji Nomura,[†] Takahiro Uno,[†] Masataka Kubo,[†] Norimitsu Tohnai,[‡] and Miki Miyata[‡]

[†]Division of Chemistry for Materials, Graduate School of Engineering, Mie University 1577 Kurima Machiya-cho, Tsu, Mie 514-8507, Japan, and [‡]Department of Material and Life Science, Graduate School of Engineering, Osaka University 2-1 Yamadaoka, Suita, Osaka 565-0871, Japan

Received May 27, 2009; Revised Manuscript Received July 30, 2009

ABSTRACT: Solid-state polymerization of 7,7,8,8-tetrakis(methoxyethoxycarbonyl)quinodimethane (**1**) was investigated *in vacuo* by irradiation using a high-pressure mercury lamp at 30 °C. The polymerization of **1** in the solid state took place in very slow rate and reached to a complete conversion at 37 days. UV irradiation of **1** crystals formed a diradical dimer of **1** as a reactive intermediate, coupling reaction of which afforded a corresponding polymer with a molecular weight of > 20 000. When the UV-irradiated **1** crystals were dissolved in a degassed solvent, a 1,1,2,2,9,9,10,10-octa(methoxyethoxycarbonyl)[2.2]paracyclophane is formed and it can react with molecular oxygen in air and/or dissolved oxygen in solvents to afford a peroxide-bridged cyclophane. The molecular packing mode of **1** in the crystals was investigated by X-ray crystal structure analysis, and the low polymerization reactivity of **1** in the solid state and the formation of 1,1,2,2,9,9,10,10-octa(methoxyethoxycarbonyl)[2.2]paracyclophane were discussed on the basis of the molecular packing mode.

Introduction

Solid-state polymerizations have been paid attention as an environmental-friendly polymerization method. Topochemical polymerization is counted as a specific case in the solid-state polymerizations and is a promising method to obtain polymers with highly controlled structures such as regioselectivity, stereoregularity, molecular weight, and so on. Since topochemical polymerization proceeds with no movement of the center of gravity of the monomer molecule and only slight rotation of the monomer molecule around the gravity, the crystallographic position and symmetry of the monomer crystals are retained in the resulting polymer crystals. Owing to such strict requirements, only a limited number of monomers such as derivatives of diacetylene,¹ 2,5-distyrylpyrazine,² triene and triacetylene,³ and muconic acid and sorbic acid⁴ have been known to undergo topochemical polymerization. Diacetylene derivatives among them have been widely investigated as the candidates for preparation of the advanced materials and supramolecular polymers on the basis of crystal engineering.⁵ Recently, in the course of the solid-state polymerization studies of 7,7,8,8-tetrakis(alkoxycarbonyl)quinodimethanes,⁶ we found that selected 7,7,8,8-tetrakis(alkoxycarbonyl)quinodimethanes could undergo topochemical polymerization, and their solid-state polymerization reactivities significantly depend upon the packing mode of the molecules in the crystals by the single crystal structure analysis based on their polymorphs. By this finding, the quinodimethane monomers have joined in a member of the topochemically polymerizable monomers. However, it is still difficult to predict and control the polymerization properties of compounds in the crystals, because arrangements of monomer molecules play a

significant role. Further investigation of the crystal structures of quinodimethane monomers with solid-state polymerization reactivity would give us important information about the strict requirements needed for the topochemical polymerization of the quinodimethane monomers that assemble in a fortunate manner. In the crystals of 7,7,8,8-tetrakis(chloroethoxycarbonyl)- and 7,7,8,8-tetrakis(bromoethoxycarbonyl)quinodimethanes,⁶ monomer molecules are aligned into the column with the requirements needed for a topochemical polymerization effectively by the CH/ π interaction between hydrogen at the 2 position in the haloethoxy group and the neighboring quinodimethane ring in the same column and halogen–halogen interaction between haloethoxy groups of quinodimethane molecules in the neighboring columns. In this work, we synthesized 7,7,8,8-tetrakis(methoxyethoxycarbonyl)quinodimethane (**1**) as a novel monomer, where methoxyethoxy group is expected to form a weak CH/O hydrogen bond interaction instead of a halogen–halogen interaction and has an electron-donating methoxy group instead of electron-accepting halogen atom, and investigated the polymerization of **1** under UV irradiation in the solid state *in vacuo*, and also the relationship of the solid-state polymerization reactivity with their crystal structures will be discussed.

Experimental Section

Materials. Benzene was washed in sequence with concentrated sulfuric acid, water, a 5% aqueous sodium hydroxide, and again water, dried over anhydrous calcium chloride, refluxed over metal sodium, and then distilled. Tetrahydrofuran (THF) was refluxed over lithium aluminum hydride for 12 h and distilled, and then the distillate was distilled again over benzophenone–sodium. 2,2'-Azobis(isobutyronitrile)(AIBN) was recrystallized from methanol. Pyridine was distilled over potassium hydroxide. Titanium tetrachloride was distilled over

*To whom correspondence should be addressed: Telephone: +81-59-231-9410. Fax: +81-59-231-9410. E-mail: itoh@chem.mie-u.ac.jp.

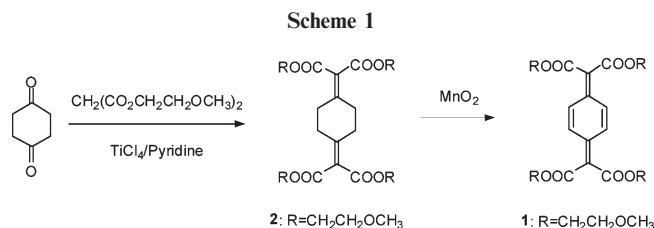
copper powder under reduced pressure. Commercial carbon tetrachloride, 2-methoxyethanol, activated manganese(IV) dioxide, and 2,2,6,6-tetramethylpiperidine 1-oxyl (TEMPO) were used without further purification.

Monomer Synthesis. Di(2-methoxyethyl) Malonate. Malonic acid (20.8 g, 200 mmol), 2-methoxyethanol (30.5 g, 400 mmol), and *p*-toluene sulfonic acid monohydrate (0.16 g, 0.82 mmol) in benzene (100 mL) were reacted at reflux for 24 h. The reaction mixture was washed with saturated sodium chloride aqueous solution (100 mL \times 2) and saturated sodium bicarbonate aqueous solution (100 mL \times 2), and then dried over anhydrous magnesium sulfate. After filtration, the solvent was evaporated under reduced pressure to give crude product, which was distilled under reduced pressure to give di(2-methoxyethyl) malonate as a colorless oil (35.2 g, 80% yield). bp 117 °C (4 mmHg). IR (NaCl, ν , cm^{-1}): 2900 (CH), 1739 (C=O), 1128 (C–O). ^1H NMR (270 MHz, CDCl_3 , δ , ppm): 4.30 (t, $J = 4.6$ Hz, 4H, CH₂), 3.61 (m, 4H, CH₂), 3.47 (s, 2H, CH₂), 3.39 (s, 6H, CH₃). ^{13}C NMR (67.7 MHz, CDCl_3 , δ , ppm): 166.1 (C=O), 69.8 (CH₂), 64.1 (CH₂), 58.5 (CH₃), 40.8 (CH₂). Anal. Calcd for $\text{C}_9\text{H}_{16}\text{O}_6$: H, 7.32; C, 49.09; O, 43.59. Found: H, 7.37; C, 48.53; O, 43.58.

1,4-Bis[di(2-methoxyethoxycarbonyl)methylene]cyclohexane (2). Titanium tetrachloride (12 mL, 146 mmol) was added dropwisely under nitrogen into dry stirred THF (220 mL) cooled in an ice bath. This gives a bright yellow precipitate after an exothermic reaction. Into this yellow mixture were added dropwisely 1,4-cyclohexanedione (2.25 g, 20.1 mmol) and di(2-methoxyethyl) malonate (8.82 g, 40.0 mmol) in THF (20 mL), and then stirred for 1 h. Pyridine (20 mL) in THF (20 mL) was added dropwisely into the resulting brown suspension over 1 h, and the reaction mixture was stirred at room temperature for 2 days. Water (150 mL) and chloroform (100 mL) were added into the reaction mixture, the organic layer was separated, and then the aqueous layer was extracted with chloroform (3 \times 100 mL). The combined organic fractions were successively washed with saturated aqueous sodium chloride (3 \times 100 mL) and aqueous sodium bicarbonate (2 \times 100 mL), dried over anhydrous magnesium sulfate, and filtered, and then the solvent of the filtrate was evaporated under reduced pressure. The crude product was purified by column chromatography (SiO_2 , chloroform/ethyl acetate (3/1, v/v)) and 1,4-bis[di(methoxyethoxycarbonyl)methylene]cyclohexane (**2**) was obtained in 7.84 g (76% yield) as yellow oil. IR (NaCl, ν , cm^{-1}): 2892 (CH), 1724 (C=O), 1634 (C=C), 1236 and 1050 (C–O). ^1H NMR (270 MHz, CDCl_3 , δ , ppm): 4.33 (m, 8H, CH₂), 3.61 (m, 8H, CH₂), 3.37 (s, 12H, CH₃), 2.77 (s, 8H, CH₂). ^{13}C NMR (67.7 MHz, CDCl_3 , δ , ppm): 164.7 (C=O), 158.6 ($> \text{C}=\text{C}$), 122.8 ($=\text{C} <$), 70.0 (CH₂), 63.8 (CH₂), 58.7 (CH₃), 29.2 (CH₂). Anal. Calcd for $\text{C}_{24}\text{H}_{36}\text{O}_{12}$: H, 7.02; C, 55.81; O, 37.17. Found: H, 7.04; C, 55.52; O, 36.98.

7,7,8,8-Tetrakis(2-methoxyethoxycarbonyl)quinodimethane (1). **2** (404 mg, 0.781 mmol) was dissolved in benzene (50 mL), and this solution was added in one portion into activated manganese dioxide (2.70 g, 31.1 mmol) in benzene (250 mL) at reflux. After stirring for 10 min at reflux, activated manganese dioxide was removed by filtration and the solvent was evaporated under reduced pressure. The crude yellow oil was purified by column chromatography (SiO_2 , chloroform/ethyl acetate (4/1, v/v) and then benzene) followed by recrystallization from dichloromethane/hexane (1/3, v/v) at -20 °C to give **1** as pale yellow plates (104 mg, 26%). Mp: 56 °C. IR (KBr, ν , cm^{-1}): 2890 (CH), 1729 (C=O), 1582 (C=C), 1241 and 1044 (C–O). ^1H NMR (270 MHz, CDCl_3 , δ , ppm): 7.49 (s, 4H, CH), 4.41 (m, 8H, CH₂), 3.64 (m, 8H, CH₂), 3.39 (s, 12H, CH₃). ^{13}C NMR (67.7 MHz, CDCl_3 , δ , ppm): 164.5 (C=O), 139.3 ($> \text{C}=\text{C}$), 130.1 ($=\text{CH}$), 125.6 ($=\text{C} <$), 70.0 (CH₂), 64.3 (CH₂), 58.8 (CH₃). Anal. Calcd for $\text{C}_{24}\text{H}_{32}\text{O}_{12}$: H, 6.29; C, 56.24; O, 37.46. Found: H, 6.30; C, 56.20; O, 37.06.

Polymerization Procedure. For the solid-state polymerization, a given amount of monomer crystals (**1**) were put in a Pyrex ampule, which was degassed under reduced pressure and



sealed. Polymerization was carried out at 30 °C under UV irradiation by using a high-pressure mercury lamp (Fuji Glass Work type HB-400, 400 W) at a distance of 12 cm for 37 days. A small amount of chloroform was added to the reaction product in the ampule and the resulting suspension was added into an excess of hexane to deposit a polymeric product as a hexane-insoluble fraction. The supernatant was placed under reduced pressure to remove the solvent and to produce a residue as a hexane-soluble fraction.

Hexane-insoluble fraction (high molecular weight polymer): white powder in 28% yield. $M_p > 20\,000$. IR (KBr, ν , cm^{-1}): 2890 (CH), 1739 (C=O), 1451 (C=C), 1248 and 1201 (C–O). ^1H NMR (270 MHz, CDCl_3 , δ , ppm): 6.74 (br, 4H, aromatic), 4.35 (br, 8H, CH₂), 3.56 (br, 8H, CH₂), 3.27 (br, 12H, CH₃). ^{13}C NMR (67.7 MHz, CDCl_3 , δ , ppm): 168.8 (C=O), 132.7 (Ar), 129.8 (Ar), 77.2 ($> \text{C} <$), 69.7 (CH₂), 65.3 (CH₂), 58.5 (CH₃). Anal. Calcd for $(\text{C}_{24}\text{H}_{32}\text{O}_{12})_n$: H, 6.29; C, 56.24; O, 37.46. Found: H, 6.33; C, 55.90; O, 37.41.

Hexane-soluble fraction (low molecular weight product): white viscous oil in 72% yield. $M_p = 700$. IR (NaCl, ν , cm^{-1}): 2892 (CH), 1747 (C=O), 1451 (C=C), 1264 and 1214 (C–O). ^1H NMR (270 MHz, CDCl_3 , δ , ppm): 6.96 (br, 8H, aromatic), 4.39 (m, 16H, CH₂), 3.62 (m, 16H, CH₂), 3.36 (s, 12H, CH₃), 3.33 (s, 12H, CH₃). ^{13}C NMR (67.7 MHz, CDCl_3 , δ , ppm): 168.8 (C=O), 164.4 (C=O), 137.1 (Ar), 133.0 (Ar), 130.4 (Ar), 128.7 (Ar), 89.4 ($> \text{C} <$), 72.1 ($> \text{C} <$), 69.7 (CH₂), 65.2 (CH₂), 58.8 (CH₃). Anal. Calcd for $\text{C}_{48}\text{H}_{64}\text{O}_{26}$: H, 6.10; C, 54.54; O, 39.35. Found: H, 6.17; C, 54.50; O, 39.04.

For the melt polymerization, **1** (205.0 mg) and AIBN (3.5 mg) as an initiator were placed in a Pyrex ampule, degassed and then sealed. The ampule was set in a bath at 60 °C for 24 h and then opened. One mL of chloroform was added into the reaction product and the resulting solution was poured into an excess of diethyl ether to deposit a polymeric product. The product was collected by centrifugation and dried under reduced pressure at room temperature until a constant weight was attained: 99.8 mg (54% yield). $M_p = 23\,000$. ^1H NMR (270 MHz, CDCl_3 , δ , ppm): 6.74 (br, 4H, aromatic), 4.35 (br, 8H, CH₂), 3.56 (br, 8H, CH₂), 3.27 (br, 12H, CH₃). ^{13}C NMR (67.7 MHz, CDCl_3 , δ , ppm): 168.8 (C=O), 132.7 (Ar), 129.8 (Ar), 77.2 ($> \text{C} <$), 69.7 (CH₂), 65.3 (CH₂), 58.5 (CH₃). Anal. Calcd for $(\text{C}_{24}\text{H}_{32}\text{O}_{12})_n$: H, 6.29; C, 56.24; O, 37.46. Found: H, 6.14; C, 55.55; O, 38.17.

Trap of Reactive Intermediate by TEMPO. Pale yellow crystals of **1** (138.7 mg) were put in a Pyrex ampule, which was degassed under reduced pressure and sealed. The ampule containing **1** was irradiated at 30 °C with a high-pressure mercury lamp for 37 days to attain complete monomer conversion. The ampule was opened in an argon-filled globe box maintained to a dew point of -95 °C to avoid contact with molecular oxygen and moisture in air. Into the ampule was added TEMPO (57.0 mg), and then it was heated at 60 °C for a few minutes. A small amount of the reaction mixture was dissolved in a chloroform-*d* degassed by freeze–thaw method in the globe box, and then ^1H NMR and ^{13}C NMR measurements were performed to characterize the reaction product.

X-ray Crystallography. The powder X-ray diffraction (XRD) measurements of monomer crystals and the UV-irradiated crystals were carried out using Rigaku Rotaflex RU-200B in the 2θ range from 5 to 60° at a scan speed of 0.5°/min with sampling width of 0.02°. The graphite-monochromated Cu K α radiation ($\lambda = 1.54178$ Å) was used with the power of the X-ray generator 40 kV and 150 mA. Single crystals were obtained as

Table 1. Polymerizations^a of **1** in the solid state and the melt and of BrEtQM in the solid state in vacuo

run no.	monomer /mg	state	light source	temp/°C	time/days	convn/%	M_p^c
1							
1	100	solid state	Hg lamp	30	24	75 ^d	> 20 000 700 300
2	100	solid state	Hg lamp	30	37	> 99 ^d	> 20 000 700
3 ^b	205	melt	dark	60	1	54	23 000
BrEtQM							
4	101	solid state	Hg lamp	30	3 min	> 99 ^d	insoluble

^a Irradiation with high pressure Hg lamp (400 W). ^b AIBN, 3.5 mg. ^c Determined by GPC measurement using THF as an eluent and standard polystyrene as a reference. ^d Determined by ¹H NMR measurement (from the amount of unreacted monomer).

plates by recrystallization from a mixture of dichloromethane/hexane (3/1, v/v) at $-20\text{ }^{\circ}\text{C}$. The crystal size is to be $0.50 \times 0.40 \times 0.05\text{ mm}$. Single-crystal X-ray diffraction data were collected on a Rigaku RAXIS-RAPID Imaging Plate diffractometer using Cu K α radiation ($\lambda = 1.54178\text{ \AA}$) monochromated with graphite. The structures were solved by the direct methods with the programs SIR88⁷ and SIR92⁸ and refined by full-matrix least-squares procedures. All calculations were performed using the TEXSAN crystallographic software package of the Molecular Structure Corporation.

Measurements. All melting points were obtained with a Yanaco MP-S3 melting point apparatus. Elemental analyses were performed on a Yanaco CHN Corder MT-5 Instruments. The molecular weights (M_n) of the polymers were estimated by gel permeation chromatography (GPC) on a JASCO PU-2080 Plus equipped with TOSOH UV-8020 ultraviolet (254 nm) detector and TSK gel G2500H₈ (bead size with $10\text{ }\mu\text{m}$, molecular weight range 1.0×10^2 to 2.0×10^4) and TSK gel G3000H₈ (bead size with $10\text{ }\mu\text{m}$, molecular weight range 1.0×10^2 to 6.0×10^4) using THF as an eluent at a flow rate of 1.0 mL/min and polystyrene standards for calibration. ¹H NMR and ¹³C NMR spectra were recorded on a JEOL JNM-EX 270 FT NMR spectrometer in chloroform-*d* with tetramethylsilane as an internal standard, and infrared (IR) spectra were recorded on a JASCO FT/IR-4100 spectrometer. Differential scanning calorimetry measurement (DSC) and thermogravimetric analysis (TGA) of the products were performed on a Seiko DSC 6220 and TG/DTA 6200 Instruments at a scan speed of $+5\text{ }^{\circ}\text{C/min}$ under nitrogen gas flow.

Results and Discussion

Monomer Synthesis and Crystallization. The synthetic route of monomer crystals (**1**) is shown in Scheme 1.

Knoevenagel condensation of 1,4-cyclohexanedione with di(2-methoxyethyl) malonate using titanium tetrachloride and pyridine as a dehydrating system⁹ gave **2** in 76% yield as yellow viscous oil. Oxidations of **2** with activated manganese dioxide in benzene heated at reflux and subsequent purification by column chromatography treatment gave **1** in 26% yield. Pale yellow plate crystals were obtained by recrystallization from a dichloromethane/hexane (1/3, v/v) solution at $-20\text{ }^{\circ}\text{C}$ and used for polymerization. The chemical structure of **1** was confirmed by IR, ¹H NMR, ¹³C NMR, and elemental analysis. During crystallization of **1**, we found that relatively rapid evaporation of diethyl ether solution and of dichloromethane/hexane (1/20 v/v) solution at room temperature provided pale yellow plate crystals, and rapid evaporation of diethyl ether solution at a refrigerator at $-20\text{ }^{\circ}\text{C}$ provided colorless plate crystals, which were changed to yellow crystals at room temperature, indicating of some sort of phase transition. The detailed phase transition behavior will be published elsewhere.

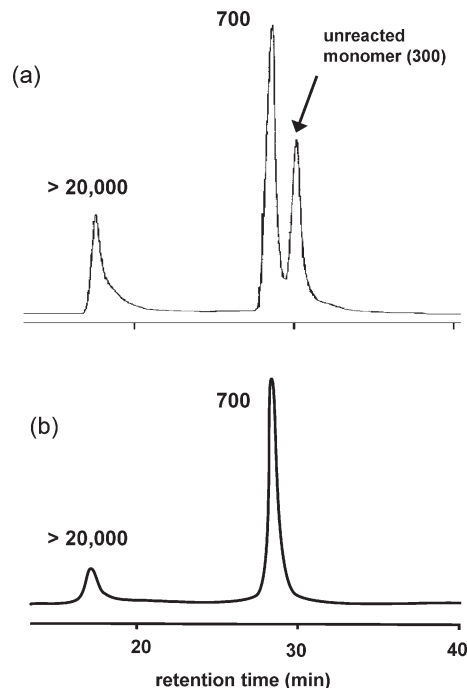


Figure 1. GPC charts of UV-irradiated **1** crystals for (a) 24 days and (b) 37 days, respectively.

Polymerization and Polymer Characterization. Polymerization of **1** was performed in the solid state by UV irradiation with a high-pressure mercury lamp *in vacuo* at $30\text{ }^{\circ}\text{C}$ for 24 and 37 days, and in the melt state in the presence of AIBN at $60\text{ }^{\circ}\text{C}$ for one day, and the results are summarized in Table 1, together with previous result of the solid-state polymerization of 7,7,8,8-tetrakis(bromoethoxycarbonyl)quinodimethane (**BrEtQM**),⁶ which could polymerize topochemically, for comparison.

When the plate crystals of **1** were exposed to UV light at $30\text{ }^{\circ}\text{C}$ *in vacuo*, yellow color of the crystals faded very slowly to afford white crystals with small cracks in 37 days. This indicates that polymerization rate of **1** in the solid state is very slow compared with that of **BrEtQM** crystals, yellow color of which faded completely in three minutes on exposure to UV light to afford polymer crystals with pink color.⁶ The products obtained by UV irradiation for 24 and 37 days were dissolved in a small amount of THF and their molecular weights were determined by GPC measurement. The GPC charts for 24 and 37 days are shown in Figure 1.

Three peaks (M_p : > 20 000, 700, and 300) are observed in 24 days and two peaks (M_p : > 20 000 and 700) in 37 days, respectively, and the peak at the molecular weight of 300 in

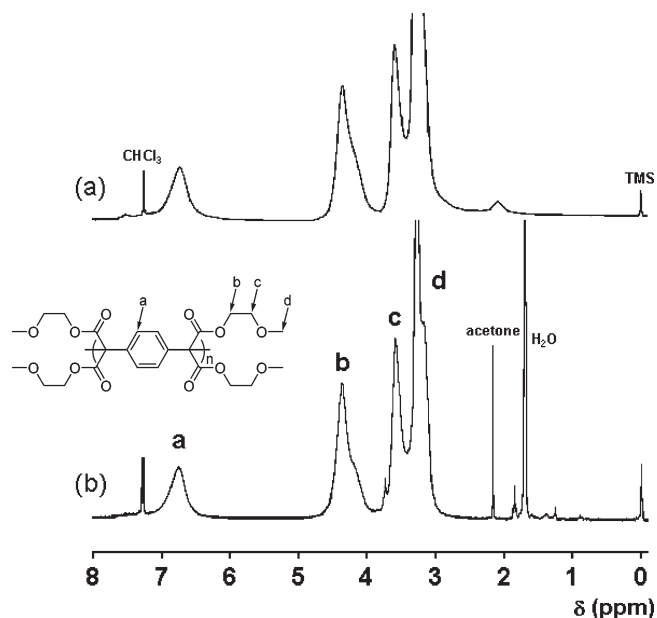


Figure 2. ^1H NMR spectra in chloroform- d of (a) hexane-insoluble part (high molecular weight product) and (b) a polymer of **1** obtained by melt polymerization in the presence of AIBN (run no. 3 in Table 1).

24 days, corresponding to the molecular weight of monomer **1**, disappeared completely in 37 days, indicating the complete conversion of monomer **1** under UV irradiation in 37 days. The molecular weight of 700 for a low molecular weight product observed in 24 and 37 days is close to that of the dimer of **1**. Here, in order to characterize the reaction product, each product in 37 days, a high molecular weight product ($> 20\,000$) and a low molecular weight one (700), was isolated by dissolution–precipitation method using chloroform as a solvent and hexane as a precipitant. The high molecular weight product was obtained as white powder in 28% yield as a hexane-insoluble part and the low one was obtained in white viscous oil in 72% yield as a hexane-soluble part, respectively. ^1H NMR and ^{13}C NMR spectra of the hexane-insoluble part (high molecular weight product) are shown in part a of Figures 2 and 3, respectively, which are in good agreement with those (part b in Figures 2 and 3) of a homopolymer ($M_p = 23\,000$) of **1** obtained by the melt polymerization in the presence of AIBN at $60\text{ }^\circ\text{C}$, where each peak could be assigned to respective protons and carbons of the chemical structures illustrated therein.

And also, elemental analysis values (H, 6.33; C, 55.90; O, 37.41) of the hexane-insoluble part (high molecular weight product) are in good agreement with the calculated values (H, 6.29; C, 56.24; O, 37.46) of **1**. Therefore, it is concluded that the hexane-insoluble part (high molecular weight product) obtained by UV irradiation of **1** in the solid state is to be a homopolymer of **1**.

^1H NMR and ^{13}C NMR spectra of the hexane-soluble part (low molecular weight product of 700) are shown in Figure 4, where each peak can be assigned to the respective protons and carbons of the chemical structures illustrated therein.

In the ^1H NMR spectrum, two singlet peaks assigned to methoxy protons are observed at 3.36 (e) and 3.33 (f) ppm. In the ^{13}C NMR spectrum, two peaks assigned to a carbonyl carbon are observed at 168.6 (A) and 164.4 (B) ppm, and two kinds of methine carbon (D and E) and quarternary carbon (C and F) are observed for the aromatic ring, and, moreover, quarternary carbons at the benzyl position are observed at 89.4 (G) and 72.1 (H) ppm, respectively. These peaks

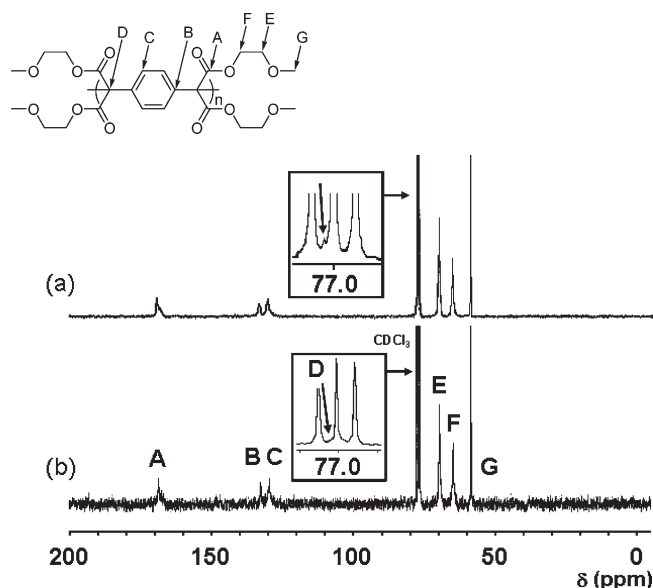


Figure 3. ^{13}C NMR spectra in chloroform- d of (a) hexane-insoluble part (high molecular weight product) and (b) a polymer of **1** obtained by melt polymerization in the presence of AIBN (run no. 3 in Table 1).

strongly suggest the chemical structure illustrated in the figure. TGA measurement showed that the hexane-soluble part (low molecular weight product of 700) begins to decompose at $119\text{ }^\circ\text{C}$, and also exothermic peak was observed at $108\text{ }^\circ\text{C}$ by DSC measurement. This behavior is similar to the thermal behavior for the alternating copolymer of 7,7,8,8-tetrakis(ethoxycarbonyl)quinodimethane with molecular oxygen reported previously.⁶ These thermal analysis indicates that the low molecular weight product might contain a peroxide bond. Moreover, elemental analysis values (H, 6.17; C, 54.50; O, 39.04) of the hexane-soluble part (the low molecular weight product) are in good agreement with the calculated values (H, 6.10; C, 54.54; O, 39.35) of a peroxide-bridged cyclophane illustrated in the figure. It is, therefore, concluded that the hexane-soluble part (low molecular weight product) obtained by UV irradiation of **1** in the solid state is a peroxide-bridged cyclophane. Unfortunately, we failed to obtain the peroxide-bridged cyclophane crystals though its crystallization was attempted under various conditions. Here, it is speculated that the peroxide-bridged cyclophane isolated as low molecular weight product is formed by reaction of [2.2]paracyclophane of **1**, 1,1,2,2,9,9,10,10-octa(methoxyethoxycarbonyl)[2.2]paracyclophane, with molecular oxygen in air and/or dissolved oxygen in solvents used during isolation process of the reaction products. To confirm this speculated reaction, we carried out the following experiment: after UV exposure on **1** in the solid state for 37 days, the irradiated **1** crystals were dissolved in chloroform- d degassed by freeze–thaw method and in an argon-filled globe box to avoid contact with molecular oxygen in air, and then the resulting solution was contacted with oxygen gas and the spectral changes in the ^1H NMR and ^{13}C NMR spectra were monitored in a given interval time. ^1H NMR and ^{13}C NMR spectra just after dissolving the UV-irradiated **1** crystals are shown in (b) of Figure 5, together with those of monomer **1** (part a in Figure 5).

In the ^1H NMR spectrum, four peaks are observed at 6.79 (br, 8H) (a'), 4.41 (m, 16H) (b'), 3.65 (t, $J = 4.95$, 16H) (c'), and 3.34 (s, 24H) (d') ppm. Peaks assigned to the methoxy protons at 3.34 (d') ppm and to the aromatic ring protons at 6.79 (a') ppm are observed as a singlet peak and a broad singlet peak, respectively. In the ^{13}C NMR spectrum, six

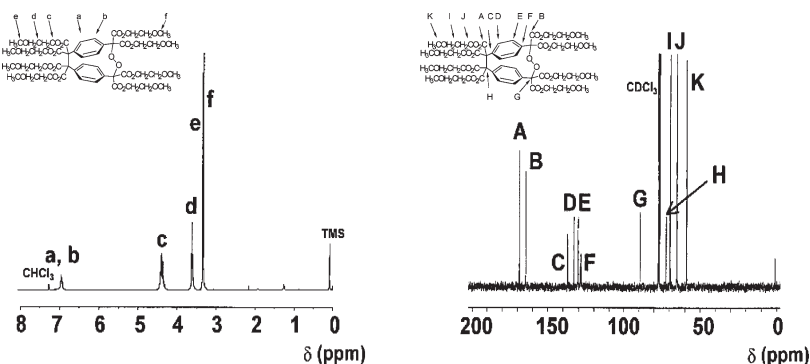


Figure 4. ^1H NMR and ^{13}C NMR spectra in chloroform-*d* of the hexane-soluble part (low molecular weight product of 700).

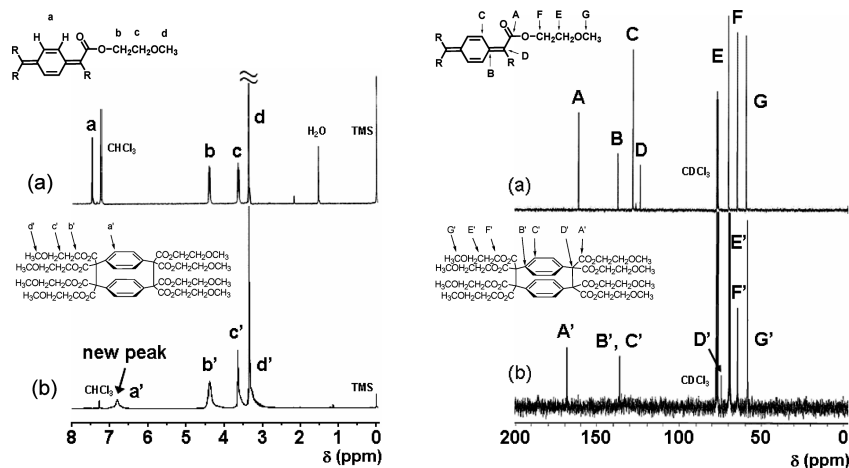


Figure 5. ^1H NMR and ^{13}C NMR spectra in chloroform-*d* of (a) monomer crystals **1** and (b) UV-irradiated **1** crystals just after dissolving.

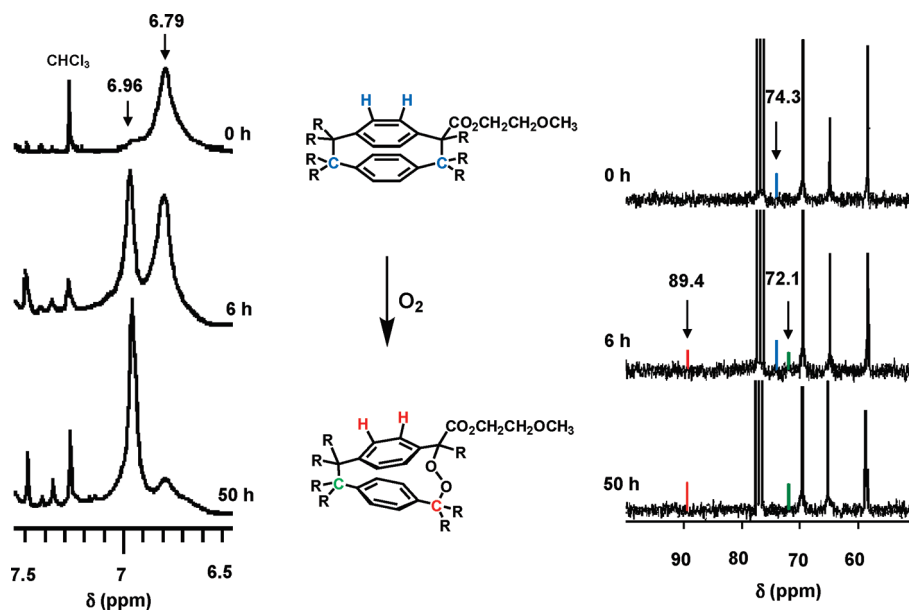


Figure 6. Spectral changes in ^1H NMR and ^{13}C NMR spectra in chloroform-*d* for the reaction with oxygen gas at 0, 6, and 50 h.

peaks are observed at 168.8 (C=O) (A'), 136.2 (Ar) (B' and C'), 74.3 (>C<) (D'), 69.8 (CH₂) (E'), 65.2 (CH₂) (F'), and 58.8 (CH₃) (G') ppm, respectively. The peak at 168.6 (A') ppm is assigned to a carbonyl carbon and is observed as a single peak for carbonyl group, the peak at 136.2 (B' and C') ppm is assigned to methine and quaternary carbons in the aromatic ring and is observed as a single peak owing to peak overlapping, and the peak at 74.3 (D') ppm is assigned to

quaternary carbon at the benzyl position and is observed as a single peak, respectively. Other peaks in the figure are assigned well to the protons and carbons of the chemical structure illustrated therein. Therefore, these peaks strongly suggest the formation of [2.2]paracyclophane of **1**, 1,1,2,2,9,9,10,10-octa(methoxyethoxycarbonyl)[2.2]paracyclophane. The spectral changes of the aromatic proton region (7.5–6.5 ppm) in the ^1H NMR spectrum and of the aliphatic

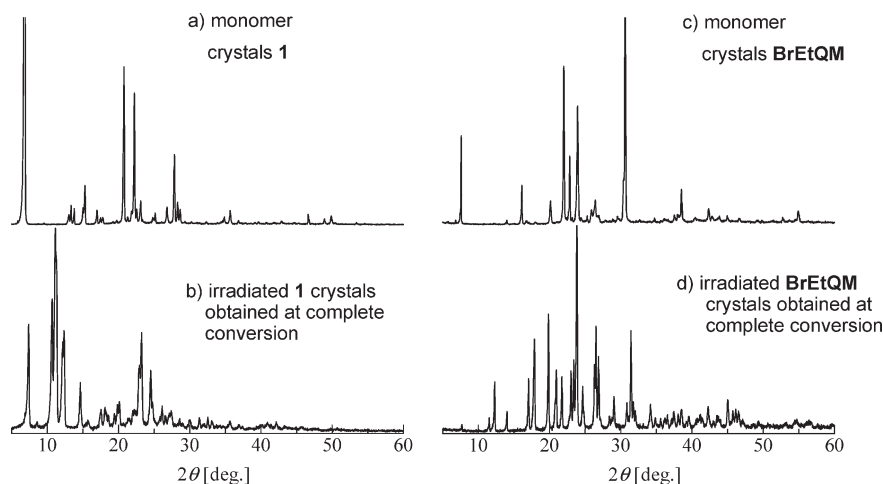


Figure 7. XRD patterns of (a) monomer crystals **1**, (b) UV-irradiated **1** crystals, (c) monomer crystals **BrEtQM**, and (d) UV-irradiated **BrEtQM** crystals.

carbon region (50–100 ppm) in the ^{13}C NMR spectrum for the reaction with oxygen gas are shown in Figure 6, respectively.

In the ^1H NMR spectrum at 6 h, in addition to peak at 6.79 ppm due to the aromatic protons in 1,1,2,2,9,9,10,10-octa-(methoxyethoxycarbonyl)[2.2]paracyclophane, a new peak appeared at 6.96 ppm, and at 50 h it increased largely, but the peak at 6.79 ppm decreased. As an additional spectral change, a new singlet peak, which is the next to a singlet peak at 3.34 ppm, appeared at 3.36 ppm, assigned to the methoxy group in the peroxide-bridged cyclophane. In the ^{13}C NMR spectrum at 6 h, in addition to peak at 74.3 ppm due to the quaternary carbons at the benzyl position (bridge head) in the 1,1,2,2,9,9,10,10-octa-(methoxyethoxycarbonyl)-[2.2]paracyclophane, new two peaks appeared at 89.4 and 72.1 ppm, assigned to quaternary carbons at the benzyl position of the peroxide-bridged cyclophane, and at 50 h the peak at 74.3 ppm disappeared completely and only new two peaks at 89.4 and 72.1 ppm are observed. As an additional spectral change, peaks assigned to carbonyl group were observed at 168.6 and 164.4 ppm, and peaks assigned to aromatic ring carbons were observed at 137.1, 133.0, 130.4, and 128.7 ppm in 50 h. The ^1H NMR and ^{13}C NMR spectra observed in 50 h are completely in good agreement with those of peroxide-bridged cyclophane. These spectral changes strongly support that 1,1,2,2,9,9,10,10-octa-(methoxyethoxycarbonyl)[2.2]paracyclophane reacts with molecular oxygen to form a peroxide-bridged cyclophane. It is, therefore, concluded that the peroxide-bridged cyclophane isolated as a low molecular weight product is formed by the reaction of 1,1,2,2,9,9,10,10-octa-(methoxyethoxycarbonyl)[2.2]paracyclophane with molecular oxygen in air and/or dissolved oxygen in solvent during the isolation process of the reaction products, and high reactivity of 1,1,2,2,9,9,10,10-octa-(methoxyethoxycarbonyl)[2.2]paracyclophane is considered to originate in its strained structure.¹⁰

Crystal Structure and Packing of Molecules. The powder X-ray diffraction (XRD) patterns of monomer crystals **1** and irradiated **1** crystals obtained at complete conversion under UV irradiation *in vacuo* are shown in a) and b), respectively, in Figure 7, together with those of monomer **BrEtQM** crystals and irradiated **BrEtQM** crystals obtained at complete conversion under same conditions.

The sharp diffraction patterns of UV-irradiated **1** crystals obtained in 37 days and of UV-irradiated **BrEtQM** crystals obtained in 3 min indicate that both monomers crystals show

Table 2. Crystallographic Data for the Crystals of **1** and **BrEtQM**

parameter	1	BrEtQM
substituent	$\text{MeOCH}_2\text{CH}_2$	BrCH_2CH_2
formula	$\text{C}_{12}\text{H}_{16}\text{O}_6$	$\text{C}_{24}\text{H}_{20}\text{Br}_4\text{O}_8$
formula wt	256.25	707.99
crystal system	monoclinic	triclinic
space group	$P2_1/a$	$P\bar{1}$
a , Å	8.073(1)	6.961(3)
b , Å	13.137(2)	7.815(4)
c , Å	13.087(2)	12.232(5)
α , deg	90	102.80(3)
β , deg	103.371(4)	97.14(2)
γ , deg	90	106.15(3)
V , Å ³	1350.3(3)	610.9(5)
Z	4	1
ρ_{calc} , g/cm ³	1.260	1.924
no. of unique reflns	2460	1945
no. obsd reflns	15428	4300
R , R_w	0.162, 0.168	0.212, 0.392
R_1	0.058	0.126
GOF	0.69	3.24
$2\theta_{\text{max}}$, deg	136.5	136.3
temp, °C	0	−70

no loss of crystallinity before and after completion of the reaction. The signal positions in the powder XRD patterns at complete conversion of **BrEtQM** are in fairly good agreement with those of monomer **BrEtQM** crystals, due to the progress of the topochemical polymerization for **BrEtQM** as reported previously.⁶ On the other hand, the signal positions in the powder XRD patterns of UV-irradiated **1** crystals obtained in 37 days are significantly different from those of monomer **1** crystals, suggesting formation of some kinds of highly crystalline compounds.

To clarify the molecular packing modes of **1** and **BrEtQM** in the crystals and the drastic difference between the abilities of **1** and **BrEtQM** to undergo polymerization, we investigated the crystal structures of both monomers by X-ray crystallography. The crystallographic data of both **1** and **BrEtQM** are summarized in Table 2, and their crystal structures are shown in Figure 8.

In the crystal structures of **1** and **BrEtQM**, both crystals construct a similar one-dimensional columnar structure by the stacking of the quinodimethane rings along the crystallographic a axis, and also the stacking axis is not perpendicular to the molecular plane of the quinodimethane ring. Here, we examined the stacking manners in the columnar structures by structural parameters (θ_1 , θ_2 , d_s , and d_{cc}) used

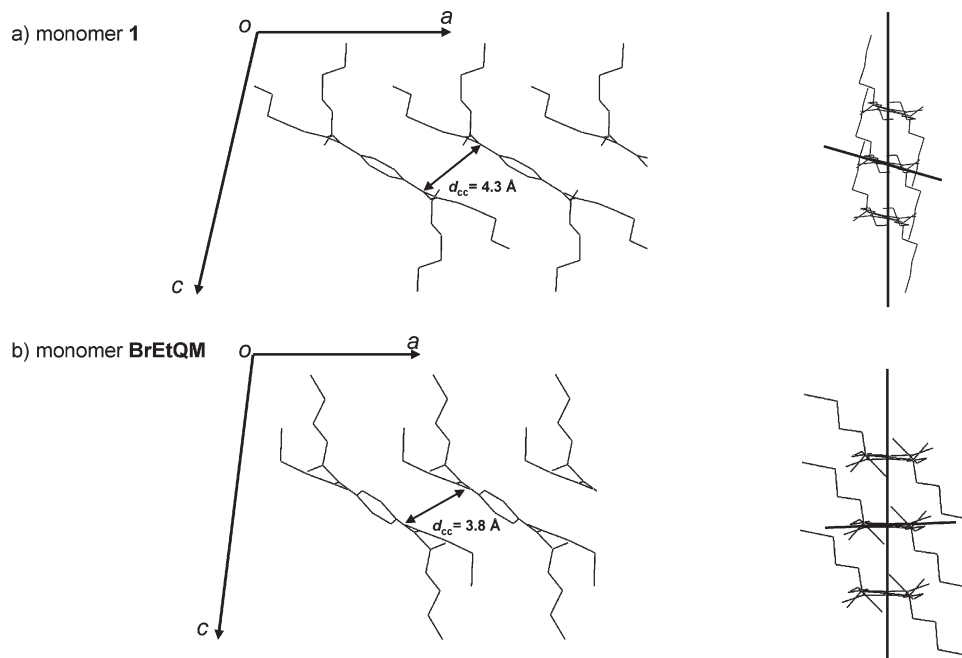
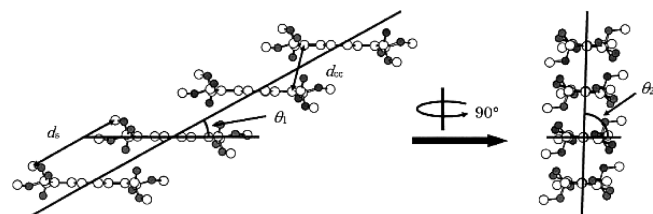


Figure 8. Crystal structures of (a) **1** and (b) **BrEtQM**. Hydrogen atoms are omitted for clarity.

Table 3. Stacking Parameters for Crystals of **1** and **BrEtQM**^a



monomer	θ_1 (deg)	θ_2 (deg)	d_{cc} (Å)	d_s (Å)
1	32	83	4.30	8.07
BrEtQM	33	89	3.84	6.99

^a θ_1 , θ_2 , tilt angles of the molecular plane; d_{cc} , distance between the reacting exomethylene carbons; d_s , stacking distance.

for monomers with planar structures such as quinodimethanes and dienes previously.^{4,6} These parameters are defined as the angles formed between the stacking axis and longer axis of the monomer molecule (θ_1) and the shorter axis of the monomer molecule (θ_2), the distance between equivalent atoms in the stacked monomers (stacking distance: d_s), and the distance between the reacting exomethylene carbons (d_{cc}). The stacking parameters of **1** and **BrEtQM** and their definitions are summarized in Table 3.

In the case of **1**, θ_1 and θ_2 are 32° and 83°, respectively, and very similar to those values ($\theta_1 = 33^\circ$ and $\theta_2 = 89^\circ$) of **BrEtQM**. However, a stacking distance ($d_s = 8.07$ Å) between the adjacent quinodimethane molecules in a column and a distance between the reacting exomethylene carbons ($d_{cc} = 4.30$ Å) in the **1** crystals are longer than those of **BrEtQM** ($d_s = 6.99$ Å and $d_{cc} = 3.84$ Å). Previously, we investigated the solid-state polymerizations of several quinodimethane monomers and examined their stacking parameters based on X-ray single crystal analysis. It was found that the topochemical polymerization could take place in the quinodimethane monomers having the crystal structures with parameters of $\theta_1 = 30\text{--}33^\circ$, $\theta_2 = 83\text{--}89^\circ$, $d_s = 7.0\text{--}7.6$ Å, and $d_{cc} = 3.8\text{--}4.2$ Å.⁶ It is reported in the topochemical polymerizations of diacetylene derivatives,¹ triene and triacetylene derivatives,³ and diene

derivatives⁴ that when the d_s value in the crystals is identical to the fiber period for the polymers, topochemical polymerization could occur easily and rapidly. It is, therefore, considered that in the solid-state polymerization of **1** under UV irradiation, very slow reaction rate of **1** in comparison with **BrEtQM** and formation of 1,1,2,2,9,9,10,10-octa-(methoxyethoxycarbonyl)[2.2]paracyclophane in degassed solution instead of polymer crystals ascribe to longer d_s and d_{cc} values for **1** in comparison with those for the topochemically polymerizable quinodimethane monomers.

Trap of Reactive Intermediate by TEMPO. Here, it is hardly considered that formation of 1,1,2,2,9,9,10,10-octa-(methoxyethoxycarbonyl)[2.2]paracyclophane in the solid-state polymerization of **1** under UV irradiation might take place in the crystals when molecules **1** are stacked in the crystals with the molecular packing mode with suitable requirements for topochemical polymerization. On the basis of the molecular stacking manner in the crystals, it is predicted that a diradical dimer of **1** would be formed as a reactive intermediate. If it was true, the diradical dimer could be trapped by TEMPO to form an adduct, which is composed of one dimer of **1** and two TEMPO as shown in Scheme 2.

Therefore, we attempted to trap a reactive intermediate in these crystals. After UV irradiation of **1** at 30 °C for 37 days, the irradiated **1** crystals were mixed with TEMPO in an argon-filled globe box to avoid contact with molecular oxygen and moisture, and then the mixture was heated at 60 °C to react for a few minutes. The reaction mixture was dissolved in degassed chloroform-*d* and the reaction product was characterized by ¹H NMR and ¹³C NMR measurements. ¹H NMR and ¹³C NMR spectra are shown in Figures 9 and 10, respectively.

No peaks assigned to 1,1,2,2,9,9,10,10-octa-(methoxyethoxycarbonyl)[2.2]paracyclophane are observed in both spectra, and each peak can be assigned quite well to the protons and carbons of the adduct, composed of one dimer of **1** and two TEMPO, illustrated therein. This indicates strongly that a diradical dimer of **1** might be produced as a reactive intermediate in the crystals **1** under UV irradiation.

Scheme 2

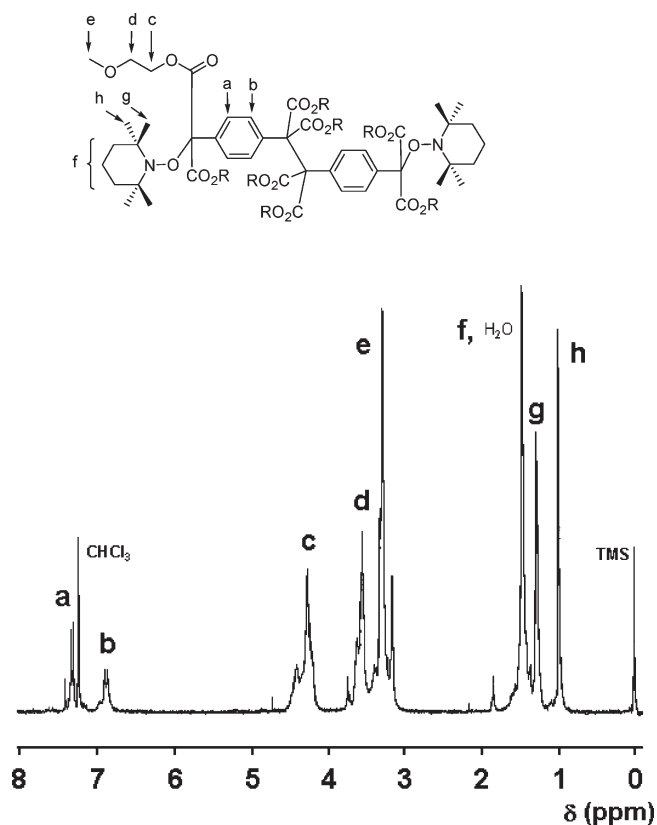
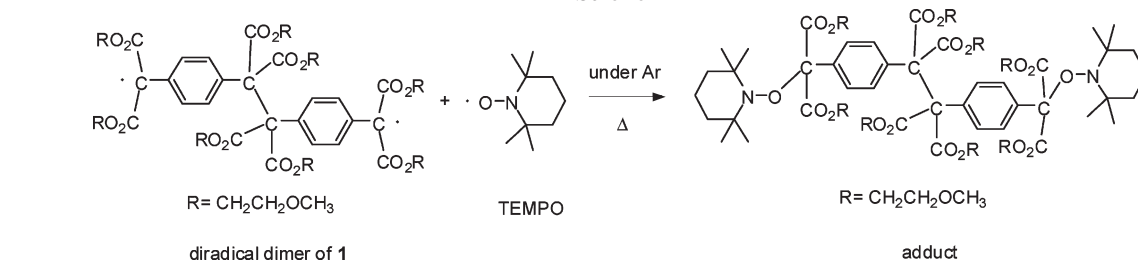


Figure 9. ¹H NMR spectrum in chloroform-*d* of the reaction mixture of the irradiated **1** crystals with TEMPO.

Reaction Mechanism. From the analysis of the reaction product of **1** after UV irradiation, trap experiment of a reactive intermediate with TEMPO, and powder X-ray diffraction and X-ray single crystal analysis of **1**, reaction process of **1** in the solid state are summarized in Scheme 3.

Monomer **1** is aligned in the crystals in accordance with the requirements needed for a topochemical polymerization like as **BrEtQM**. However, a distance (d_{cc}) between the reacting exomethylene carbons, that is, a distance between the exomethylene C7 carbon of one quinodimethane and the exomethylene C8 carbon of the neighboring quinodimethane monomer in the crystals of **1**, is longer than that of **BrEtQM**. When monomer **1** crystals were irradiated, the single bonds are formed between the reacting exomethylene carbons (for example, single bond formation in a and c positions in Scheme 3) to afford diradical dimers. The diradical dimer formation might extend a distance between the C7 carbon of one dimer and the C8 carbon of the neighboring dimer (distance in b position in Scheme 3). Owing to this extension of distance, further coupling reaction between the resulting diradical dimers is greatly suppressed in the crystals where molecular motion is greatly restricted, and, therefore, a

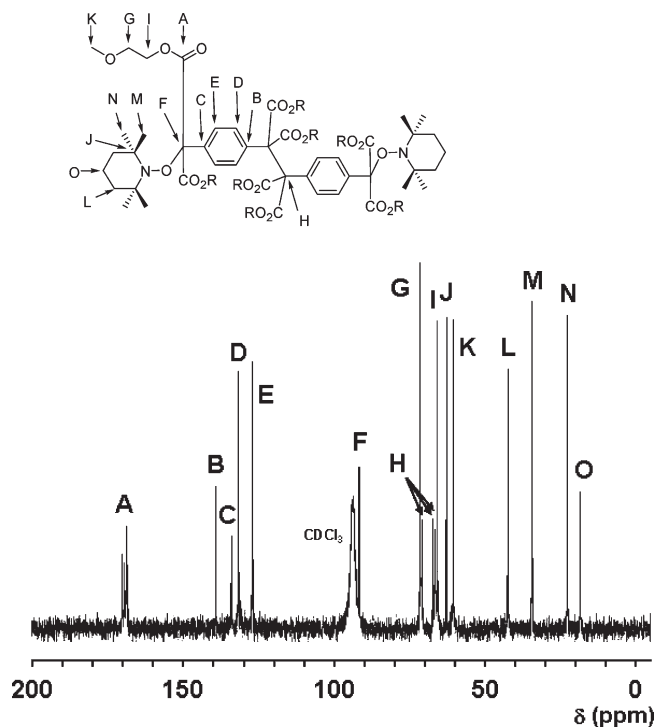
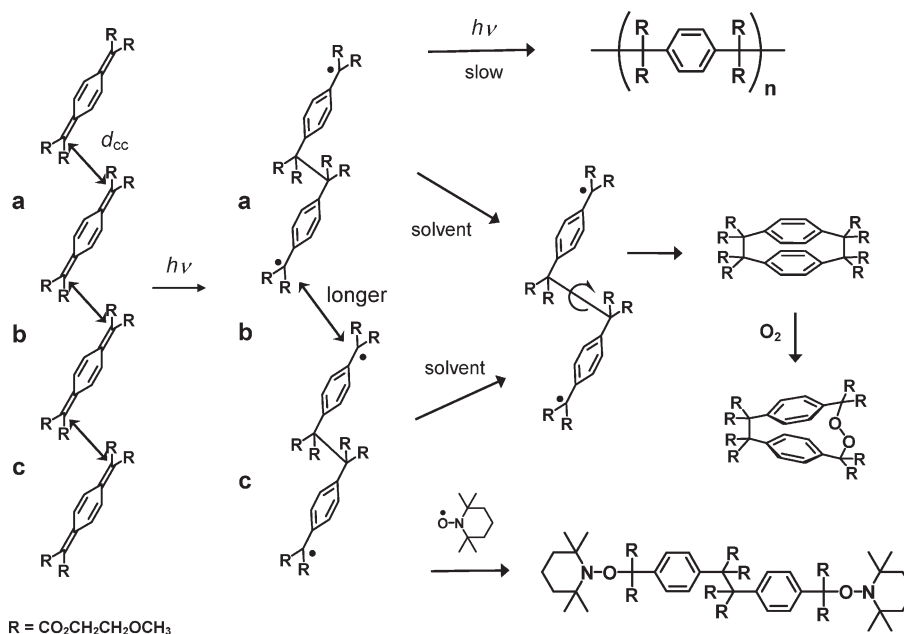


Figure 10. ¹³C NMR spectrum in chloroform-*d* of the reaction mixture of the irradiated **1** crystals with TEMPO.

reactive diradical form might be preserved as it is. Of course, in prolonged reaction time, coupling reaction of the resulting diradical dimer can take place very slowly even in the crystals due to the molecular motion, to form its polymer as shown in polymer formation of **1** under UV irradiation in 37 days. And also, when the diradical dimer formed in the crystals was dissolved in degassed chloroform-*d*, it would react intramolecularly to form 1,1,2,2,9,9,10,10-octa(methoxyethoxycarbonyl)[2.2]paracyclophane, which is unstable and can react easily with molecular oxygen in air or/and dissolved oxygen in solvents to afford the peroxide-bridged cyclophane. Moreover, the formation of an adduct composed of one dimer with two TEMPO strongly supports the presence of a reactive diradical dimer intermediate in the crystals. These findings indicate that a distance (d_{cc}) between the reacting exomethylene carbons in the crystals of **1** and a stacking distance (d_s) are close to limiting distances in requirements needed for topochemical polymerization of quinodimethane type monomers.

In summary, solid-state polymerization of **1** under UV irradiation *in vacuo* proceed very slowly to form its homopolymer via diradical dimer intermediate, which could form 1,1,2,2,9,9,10,10-octa(methoxyethoxycarbonyl)[2.2]paracyclophane when it was dissolved in degassed solvent. The 1,1,2,2,9,9,10,10-octa(methoxyethoxycarbonyl)[2.2]paracyclophane is unstable and reacts easily with molecular oxygen

Scheme 3



to form a peroxide-bridged cyclophane. From the X-ray single crystal analysis, quinodimethane molecules were aligned along the crystallographic *a* axis with a stacking distance of 8.07 Å and a distance between the reacting exomethylene carbons of 4.30 Å. In addition, the monomer molecules were stacked with a 32° tilt of the longer monomer molecule axis relative to the translational axis and with a 83° tilt of the shorter monomer molecule axis relative to the translational axis. Although the molecules are aligned in accordance with the structural requirements for a topochemical polymerization of the quinodimethane monomers, there is a slight difference, that is, the stacking distance is longer than the repeating distance in the resulting polymer, and also the distance between the reacting exomethylene carbons is longer. This structural slight difference induces slow polymerization rate of **1**.

Acknowledgment. This work was supported by Grant-in-Aid for Scientific Research (No. 18350062) from the Ministry of Education, Culture, Sports, Science, and Technology, Japan.

Supporting Information Available: X-ray crystallographic data in CIF format of **1** and **BrEtQM**. This material is available free of charge via the Internet at <http://pubs.acs.org>.

References and Notes

- (1) (a) Wegner, G. Z. *Naturforsch. B* **1969**, *24*, 824. (b) Wenger, G. *Pure Appl. Chem.* **1977**, *49*, 443. (c) Enkelmann, V. *Adv. Polym. Sci.* **1984**, *63*, 91. (d) Ogawa, T. *Prog. Polym. Sci.* **1995**, *20*, 943. (e) Coates, G. W.; Dunn, A. R.; Henling, L. M.; Dougherty, D. A.; Grubbs, R. H. *Angew. Chem., Int. Ed. Engl.* **1997**, *36*, 248. (f) Huntsman, W. D. *The Chemistry of Functional Groups, Supplement C: The Chemistry of Triple-Bonded Functional Groups*; Patai S., Rappoport Z., Eds. John Wiley & Sons: New York, 1983; Chapter 22. (g) Fomine, S.; Fomina, L.; Ogawa, T. *J. Mol. Struct. (THEOCHEM)* **2001**, *540*, 123. (h) Sandoman, D. J.; Kim, I. B.; Njus, J. M.; Lee, D. C.; Cholli, A. L.; Sahoo, S. *Macromol. Symp.* **2003**, *192*, 99. (i) Sandoman, D. J.; Njus, J. M.; Tran, B. *Macromol. Symp.* **2004**, *217*, 77. (j) Chan, Y. H.; Lin, J. T.; Chen, I. W. P.; Chen, C. H. *J. Phys. Chem. B* **2005**, *109*, 19161. (k) Xu, R.; Gramlich, V.; Frauenrath, H. *J. Am. Chem. Soc.* **2006**, *128*, 5541.
- (2) (a) Hasegawa, M. *Chem. Rev.* **1983**, *83*, 507. (b) Hasegawa, M. *Adv. Phys. Org. Chem.* **1995**, *30*, 117. (c) Coates, G. W.; Dunn, A. R.; Henling, L. M.; Ziller, J. W.; Lobkovsky, E. B.; Grubbs, R. H. *J. Am. Chem. Soc.* **1998**, *120*, 3641. (d) Pestov, D.; Levit, N.; Tepper, G. *Polymer* **2003**, *44*, 3177. (e) Levit, N.; Guney-Altay, O.; Pestov, D.; Tepper, G. *Macromolecules* **2005**, *38*, 6528.
- (3) (a) Kiji, J.; Kaiser, J.; Wegner, J. G.; Schulz, R. C. *Polymer* **1973**, *14*, 433. (b) Enkelmann, V. *Chem. Mater.* **1994**, *6*, 1337. (c) Xiao, J.; Yang, M.; Lauher, J. W.; Fowler, F. W. *Angew. Chem., Int. Ed.* **2000**, *39*, 2132. (d) Fowler, F. W.; Lauher, J. W. *J. Phys. Org. Chem.* **2000**, *13*, 850. (e) Hoang, T.; Lauher, J. W.; Fowler, F. W. *J. Am. Chem. Soc.* **2002**, *124*, 10656.
- (4) (a) Matsumoto, A.; Matsumura, T.; Aoki, S. *Macromolecules* **1996**, *29*, 423. (b) Matsumoto, A.; Yokoi, K.; Aoki, S.; Tashiro, K.; Kamae, T.; Kobayashi, M. *Macromolecules* **1998**, *31*, 2129. (c) Matsumoto, A.; Nagahama, S.; Odani, T. *J. Am. Chem. Soc.* **2000**, *122*, 9109. (d) Nagahama, S.; Matsumoto, A. *J. Am. Chem. Soc.* **2001**, *123*, 12176. (e) Matsumoto, A.; Sada, K.; Tashiro, K.; Miyata, M.; Tsubouchi, T.; Tanaka, T.; Odani, T.; Nagahama, S.; Tanaka, T.; Inoue, K.; Saragai, S.; Nakamoto, S. *Angew. Chem., Int. Ed.* **2002**, *41*, 2502. (f) Matsumoto, A.; Tanaka, T.; Tsubouchi, T.; Tashiro, K.; Saragai, S.; Nakamoto, S. *J. Am. Chem. Soc.* **2002**, *124*, 8891. (g) Matsumoto, A. *Polym. J.* **2003**, *35*, 93. (h) Oshita, S.; Matsumoto, A. *Chem.—Eur. J.* **2006**, *12*, 2139. (i) Furukawa, D.; Matsumoto, A. *Macromolecules* **2007**, *40*, 6048. (j) Matsumoto, A.; Furukawa, D.; Mori, Y.; Tanaka, J.; Oka, K. *Cryst. Growth Des.* **2007**, *7*, 1078. (k) Ueno, T.; Furukawa, D.; Matsumoto, A. *Macromol. Chem. Phys.* **2008**, *209*, 357.
- (5) (a) Okada, S.; Matsuda, H.; Nakanishi, H. *Polymeric Materials Encyclopedia*; Salamone J. C., Ed.; CRC Press: Boca Raton, FL, 1996; p 8393. (b) Bloor, D.; Chance, R. R. *Polydiacetylenes*; NATO ASI Series E, Applied Sciences No. 102; Martinus Nijhoff: Dordrecht, The Netherlands, 1985. (c) Chemls, D. S.; Zyss, J. *Non-linear Optical Properties of Organic Molecules and Crystals*; Academic Press: New York, 1987. (d) Sarkar, A. S.; Kadali, N. B.; Kamath, M. B.; Bhagmat, L. P.; Talwar, S. S. *Pure Appl. Chem.* **1999**, *A36*, 211. (e) Hwang, I. H.; Lee, S. J.; Chang, J. Y. *J. Polym. Sci.: Part A, Polym. Chem.* **2003**, *41*, 1881. (f) Dei, S.; Matsumoto, A.; Matsumoto, A. *Macromolecules* **2008**, *41*, 2467. (g) Weiss, J.; Jahnke, E.; Frauenrath, H. *Macromol. Rapid Commun.* **2008**, *29*, 330. (h) Chougrani, K.; Deschamps, J.; Dutremez, S.; Lee, A. V. D.; Barisien, T.; Lengrand, L.; Schot, M.; Filhol, J. S.; Bourry, B. *Macromol. Rapid Commun.* **2008**, *29*, 580. (i) Koevoets, R. A.; Karthikeyan, S.; Magusin, P. C. M. M.; Meijer, E. W.; Sijbesma, R. P. *Macromolecules* **2009**, *42*, 2609.
- (6) (a) Itoh, T.; Nomura, S.; Uno, T.; Kubo, M.; Sada, K.; Miyata, M. *Angew. Chem., Int. Ed.* **2002**, *41*, 4306. (b) Nomura, S.; Itoh, T.; Nakasho, H.; Uno, T.; Kubo, M.; Sada, K.; Inoue, K.; Miyata, M. *J. Am. Chem. Soc.* **2004**, *126*, 2035. (c) Nomura, S.; Itoh, T.; Ohtake, M.;

- Uno, T.; Kubo, M.; Kajiware, A.; Sada, K.; Miyata, M. *Angew. Chem., Int. Ed.* **2003**, *42*, 5468. (d) Itoh, T.; Nomura, S.; Ohtake, M.; Yoshida, T.; Uno, T.; Kubo, M.; Kajiware, A.; Sada, K.; Miyata, M. *Macromolecules* **2004**, *37*, 8230.
- (7) Burla, M. C.; Camalli, M.; Cascarano, G.; Giacovazzo, C.; Polidori, G.; Spangna, R.; Viterbo, D. *J. Appl. Crystallogr.* **1989**, *22*, 389.
- (8) Altomare, A.; Burla, M. C.; Camalli, M.; Cascarano, G.; Giacovazzo, C.; Guagliardi, A.; Polidori, G. *J. Appl. Crystallogr.* **1994**, *27*, 435.
- (9) Lehnert, W. *Tetrahedron* **1973**, *29*, 635–638.
- (10) Vögtle, F. *Cyclophane Chemistry*; John Wiley & Sons: New York, 1993; 57–215.